Cancer Research

# Sunitinib Stimulates Expression of VEGFC by Tumor Cells and Promotes Lymphangiogenesis in Clear Cell Renal Cell Carcinomas

Maeva Dufies[1], Sandy Giuliano[1,2], Damien Ambrosetti[3], Audrey Claren[1,4], Papa Diogop Ndiaye[1], Michalis Mastri[5], Walid Moghrabi[6], Lindsay S. Cooley[7], Marc Ettaiche[8], Emmanuel Chamorey[8], Julien Parola[1], Valerie Vial[2], Marilena Lupu-Plesu[1], Jean Christophe Bernhard[9], Alain Ravaud[10], Delphine Borchiellini[11], Jean-Marc Ferrero[11], Andréas Bikfalvi[7], John M. Ebos[5], Khalid Saad Khabar[6], Renaud Grépin[2], and Gilles Pagès[1]

## Abstract

Sunitinib is an antiangiogenic therapy given as a first-line treatment for renal cell carcinoma (RCC). While treatment improves progression-free survival, most patients relapse. We hypothesized that patient relapse can stem from the development of a lymphatic network driven by the production of the main growth factor for lymphatic endothelial cells, VEGFC. In this study, we found that sunitinib can stimulate *vegfc* gene transcription and increase VEGFC mRNA half-life. In addition, sunitinib activated p38 MAPK, which resulted in the upregulation/activity of HuR and inactivation of tristetraprolin, two AU-rich element–binding proteins. Sunitinib stimulated a VEGFC-dependent development of lymphatic vessels in experimental tumors. This may explain our findings of increased lymph node invasion and new metastatic sites in 30% of sunitinib-treated patients and increased lymphatic vessels found in 70% of neoadjuvant treated patients. In summary, a therapy dedicated to destroying tumor blood vessels induced the development of lymphatic vessels, which may have contributed to the treatment failure. *Cancer Res; 77(5); 1212–26. ©2017 AACR.*



## Introduction

Renal cell carcinoma (RCC) represents 85% of kidney cancers and 3% of adult cancers. However, its incidence has steadily increased. If diagnosed early, the main treatment is surgery. However, metastatic RCC has a very poor prognosis because of intrinsic resistance to radio- and chemotherapy. The main feature of RCC is hypervascularization explained by overexpression of VEGF, which is linked to mutation/inactivation of the von Hippel-Lindau (*vhl*) gene, an E3 ubiquitin ligase of the hypoxia inducible factor 1α (HIF-1α). The most widely used systemic therapy for first-line metastatic RCC is sunitinib, a tyrosine kinase inhibitor (TKI) with activity against the VEGF receptors (VEGFR1/2/3), PDGFR, CSF1R, and c-Kit (1). However, treatment benefits are transitory in most cases and the majority of patients develop resistance after one year (2). While the primary target of sunitinib is the host blood vessels via inhibition of VEGF receptors, mechanisms of resistance have been shown to stem from complex interactions between tumor and stromal cell populations (3). Indeed, several mechanisms have been proposed and can include compensatory growth factor stimulation (i.e., FGF), suppression of immunoregulatory cells, or even co-option of existing blood vessels, all of which together (or separately) could negate the impact of antivascular treatment strategies (3–6). Perhaps most provocatively, recent preclinical evidence has shown that some antiangiogenic treatments may elicit metastatic cell phenotypes, which, in turn, may also compromise tumor-reducing benefits (7, 8). Currently, more than 25 preclinical studies have confirmed this phenomena (9); however, the clinical impact is not known. Therapy-induced metastasis may explain disease progression following perioperative (adjuvant) treatment or rebound tumor growth after treatment withdrawal (10, 11).

Many studies have shown a close relationship between lymphangiogenesis, invasion, and metastasis. During tumor

[1]University of Nice Sophia Antipolis, Institute for Research on Cancer and Aging of Nice, CNRS UMR 7284, INSERM U1081, Centre Antoine Lacassagne, Nice, France. [2]Biomedical Department, Centre Scientifique de Monaco, Monaco, Principality of Monaco. [3]Central Laboratory of Pathology, Centre Hospitalier Universitaire (CHU) de Nice, Hôpital Pasteur, Nice, France. [4]Radiotherapy Department, Centre Antoine Lacassagne, Nice, France. [5]Center for Genetics and Pharmacology, Roswell Park Cancer Institute, Buffalo, New York. [6]King Faisal Specialist Hospital and Research Centre, Riyadh, Saudi Arabia. [7]University of Bordeaux, INSERM U1029, Bordeaux, France. [8]Statistics Department, Centre Antoine Lacassagne, Nice, France. [9]Service d'Urologie, Centre Hospitalier Universitaire (CHU) de Bordeaux, Bordeaux, France. [10]Service d'Oncologie Médicale, Centre Hospitalier Universitaire (CHU) de Bordeaux, Bordeaux, France. [11]Oncology Department, Centre Antoine Lacassagne, Nice, France.

**Note:** Supplementary data for this article are available at Cancer Research Online (http://cancerres.aacrjournals.org/).

S. Giuliano, D. Ambrosetti, A. Claren, P.D. Ndiaye contributed equally to this article.

R. Grépin and G. Pagès codirected the work.

**Corresponding Author:** Gilles Pagès, University Nice-Sophia Antipolis CNRS UMR 7284, INSERM U1081, 28 Avenue Valrose, Nice 06103, France. Phone/Fax: 334-9203-1231; E-mail: gpages@unice.fr

**doi:** 10.1158/0008-5472.CAN-16-3088

development, the lymphatic system is considered one of the primary routes of tumor cell dissemination that leads to distant metastatic growth. VEGFC is currently the best characterized lymphangiogenic factor that acts via VEGFR3 (12). In normal adult tissues, VEGFR3 expression is largely restricted to lymphatic endothelial cells (LEC) and its activation is responsible for LEC proliferation, migration, and survival. However, VEGFR3 is also expressed on angiogenic blood vessels (13). Several reports indicate that VEGFC expression in cancer cells correlates with accelerated tumor progression and/or an unfavorable clinical outcome (14). VEGFC overexpression in breast cancers has been shown to correlate with lymphangiogenesis and metastasis (15). In preclinical models of RCC, endothelial cells chronically exposed to an anti-VEGF antibody proliferate in response to VEGFC stimulation, whereas naïve endothelial cells are unable to do so (16). Moreover, in a preclinical model of lung cancer, resistance to aflibercept (a decoy receptor for VEGF and PlGF) is related to an increase in VEGFC (17). The VEGFC mRNA has a long 3′ untranslated domain (3′UTR) containing an adenylate and uridylate-rich element (ARE). ARE elements are binding sites for the embryonic lethal abnormal vision (ELAV) protein, also named HuR (Hu antigen R) and tristetraprolin (TTP), also named ZFP36 (zinc finger protein 36). These mRNA-binding proteins have been described previously as mRNA-stabilizing and -destabilizing factors, respectively. HuR stabilizes the mRNA of cell-cycle regulators, growth, inflammatory, and angiogenesis factors including VEGF (18). These features give HuR an oncogenic status (19). TTP has an opposite role (destabilization of these ARE-mRNA including VEGF), hence acting as a potent tumor suppressor (20). The ERK and MAPK p38 phosphorylate HuR and TTP. While ERK and p38-dependent phosphorylation activate the mRNA-stabilizing activity of HuR, phosphorylation has an opposite effect on TTP. The balance between TTP and HuR will determine mRNA stabilization or degradation (21). Although VEGFC plays a causal role in lymphangiogenesis and lymphatic metastasis, little is known about VEGFC regulation in tumor cells in response to cancer therapies.

In this study, we describe a molecular mechanism linking sunitinib treatment to lymphangiogenesis activation through the stimulation of *vegfc* gene transcription and stabilization of VEGFC mRNA. We found that VEGFC upregulation correlated with the development of a lymphatic network both in tumors in mice and in patients. Our findings suggest that antiangiogenic benefits of sunitinib may be compromised by stimulation of lymphatic vessel formation and explain compensatory prometastatic behaviors that may compromise treatment efficacy.

## Materials and Methods

### Reagents and antibodies

Sunitinib, axitinib, everolimus, pazopanib, regorafenib, sorafenib, SB203580, and PD184352 were purchased from Selleckchem. Anti-HSP90 and anti-HSP60 antibodies were purchased from Santa Cruz Biotechnology. Anti-p38, anti-phospho-p38, anti-ERK, and anti-phospho-ERK antibodies were from Cell Signaling Technology. TTP and HuR antibodies are home-made and were generated as described previously (22). DAPI, DMSO, and 5,6-Dichlorobenzimidazole 1-β-D-ribofuranoside (DRB) were purchased from Sigma-Aldrich.

### Cell culture

RCC4 (R4), ACHN (A), Caki-2 (C2), 786-0 (786) and A-498 (498) RCC cell lines, human embryonic kidney (HEK293), RAW 264.7 (RAW) macrophage cell lines were purchased from the ATCC (March 3, 2013). Stocks were made at the original date of obtaining the cells, and were usually passaged for no more than 4 months. These cell lines have been authenticated by DNA profiling using 8 different and highly polymorphic short tandem repeat loci (DSMZ). RCC10 (R10) were a kind gift from Dr. W.H. Kaelin (Dana-Farber Cancer Institute, Boston, MA). Primary cells were already described and cultured in a medium specific for renal cells (PromoCell; ref. 23).

### Immunoblotting

Cells were lysed in buffer containing 3% SDS, 10% glycerol, and 0.825 mmol/L $Na_2HPO_4$. Thirty to 50 μg of proteins were separated on 10% SDS-PAGE, transferred onto a polyvinylidene difluoride membrane (Immobilon, Millipore) and then exposed to the appropriate antibodies. Proteins were visualized with the ECL system using HRP-conjugated anti-rabbit or anti-mouse secondary antibodies.

### Quantitative real-time PCR experiments

One microgram of total RNA was used for the reverse transcription, using the QuantiTect Reverse Transcription Kit (Qiagen), with blend of oligo (dT) and random primers to prime first-strand synthesis. SYBR Master Mix Plus (Eurogentec) was used for quantitative real-time PCR (qPCR). The mRNA level was normalized to 36B4 mRNA. For oligo sequences, also see Supplementary Materials.

### Tumor xenograft experiment

***Ectopic model of RCC.*** Five million 786-O cells were injected subcutaneously into the flank of 5-week-old nude (nu/nu) female mice (Janvier). The tumor volume was determined with a caliper ($v = L \times l^2 \times 0.5$). When the tumor reached 100 $mm^3$, mice were treated 5 days a week for 4 weeks, by gavage with placebo (dextrose water vehicle) or sunitinib (40 mg/kg). This study was carried out in strict accordance with the recommendations in the Guide for the Care and Use of Laboratory Animals. Our experiments were approved by the "Comité National Institutionnel d'Éthique pour l'Animal de Laboratoire (CIEPAL)" (reference: NCE/2013-97).

***Orthotopic model of RCC.*** Tumor samples were obtained from previously published studies involving neoadjuvant sunitinib treatment in an ortho-surgical model (orthotopic tumor cell implantation followed by surgical tumor removal) of RCC (animal protocols, approvals, cell origins, and results have been previously; ref. 24). Briefly, human kidney SN12PM6$^{LUC+}$ cells ($2 \times 10^6$), were implanted into the kidney (subcapsular space) of 6 to 8weekold female CB17 SCID and treated for 14 days with sunitinib (60 mg/kg/day) prior to nephrectomy.

### Immunofluorescence

Tumor sections were handled as described previously (22, 25). Sections were incubated with DAPI, anti-mouse LYVE-1 polyclonal (Ab 14817, Abcam), or monoclonal

anti-α-smooth muscle actin (α-SMA, A2547, Sigma), and rat monoclonal anti-mouse CD31 (clone MEC 13.3, BD Pharmingen) antibodies.

### IHC

Samples were collected with the approval of the Local Ethics committee. Sections from blocks of formalin-fixed and paraffin-embedded tissue were examined for immunostaining for podoplanin, CD31, p-p38, αSMA, and LYVE1. After deparaffinization, hydration, and heat-induced antigen retrieval, the tissue sections were incubated for 20 minutes at room temperature with monoclonal anti-podoplanin, anti p-p38, anti αSMA, and anti LYVE1 antibodies diluted at 1:100. Biotinylated secondary antibody (DAKO) was applied and binding was detected with the substrate diaminobenzidine against a hematoxylin counterstain.

### Measurement of cytokines

After stimulation, cell supernatant was recovered for VEGFC measurement using the Human DuoSet ELISA kit (R&D Systems).

### Luciferase assays

Transient transfections were performed using 2 μL of lipofectamine (Gibco BRL) and 0.5 μg of total plasmid DNA-*Renilla* luciferase in a 500 μL final volume. The firefly control plasmid was cotransfected with the test plasmids to control for the transfection efficiency. Twenty-four hours after transfection, cell lysates were tested for *Renilla* and firefly luciferase. All transfections were repeated four times using different plasmid preparations. LightSwitch Promoter Reporter VEGFC (S710378) and LightSwitch 3′UTR reporter VEGFC (S803537) were purchased from Active Motif. The short and long forms of the VEGFC promoter are a kind gift of Dr. Heide L. Ford (University of Colorado School of Medicine, Aurora, CO) and Kari Alitalo (Faculty of Medicine, Biomedicum Helsinki, University of Helsinki, Helsinki, Finland; ref. 15).

### Fluorescence assays

***ARE reporter constructs and reporter activity.*** RPS30 promoter-linked EGFP reporter expression vectors containing the 3′ UTR with VEGFC ARE (5′GATTTCTTTAAAAGAATGACTATATAATTTATTTCC-3′) was constructed by inserting annealed synthetic complementary oligonucleotides with *Bam*HI and *Xba*I overhangs into the same sites of the stable control bovine growth hormone (BGH) 3′ UTR of the plasmid. The mutant ARE form was similarly constructed in which ATTTA was mutated to ATCTA (26).

***Functional response of the VEGFC ARE.*** Tetracycline-inducible (Tet-On) TTP-expressing constructs were used as described previously (26). HEK293 Tet-On Advanced cells (Clontech) were transfected with 50 ng of either the wild-type or mutant VEGFC 3′UTR reporters along with a normalization control represented by red fluorescent protein expression plasmid, and 10 ng of the TetO-TTP constructs. Transfections were performed using Lipofectamine 2000 (Invitrogen) according to the manufacturer's instructions. Doxycycline (0.25 μg/mL) was added to the transfected cells for 16 hours and fluorescence was acquired by imaging and quantified by the ProXcell imaging segmentation and quantification software.

### RNA immunoprecipitation

HEK-293 cells were transfected overnight with 2 μg vector expressing HA-tagged TTP or myc-tagged HuR. Cells were lysed in RNA IP buffer [100 mmol/L KCl, 5 mmol/L $MgCl_2$, 10 mmol/L HEPES (pH 7.0), 0.5% NP40], freshly supplemented before use with 1 mmol/L DTT, 5 μL/mL units RNase Out (Invitrogen) and protease inhibitor cocktail 1× (Roche). The lysate was centrifuged for 10 minutes at 12,000 rpm, and the supernatant was transferred to new tubes with either monoclonal anti-myc antibody or monoclonal anti-HA antibody (coupled with Protein G-sepharose beads). The beads were washed with RNA IP buffer. Aliquots were collected for immunoblotting and the remaining beads were subjected to total RNA extraction using TRI Reagent (Sigma), followed by chloroform and isopropanol precipitation. Preswollen protein-G agarose beads (GE Healthcare) were prepared by washing in PBS buffer and incubating with the antibody, followed by PBS washing. For HA-tagged TTP lysates, anti-myc–coupled beads were used as a negative control. For myc-tagged HuR lysates, anti-HA–coupled beads were used as a negative control. cDNA was synthesized from 500 ng RNA using SuperScript II Reverse Transcriptase (Invitrogen). qPCR was performed in multiplex reaction using the C1000 thermal cycler (Bio-Rad). FAM-labeled TaqMan probes (Metabion) for human VEGF-A (forward primer, 5′-AGAAGGAGGAGGGCAGAATC-3′; reverse primer, 5′-TCTCGATTGGATGGCAGTAG-3′; and TaqMan probe, 5′-Fam-CATCCAT GAACTTCACC ACTTCGTGA-BHQ-1-3′ and for human VEGF-C (forward primer: 5′-GGATGCTG-GAGAT GACTCAA-3′; reverse primer: 5′-TTCATCCAGCTCC-TTGTTTG-3′ and TaqMan probe: 5′-Fam-TCCACAGATGTCAT-GGAATCCATCTG- BHQ-1-3′ were used. VIC-labeled Ribosomal Protein (PO) probe was multiplexed with FAM-labeled probes as the endogenous control to normalize for the levels of the genes of interest.

### 5,6-Dichlorobenzimidazole riboside pulse chase experiments

DRB (25 μg/mL) was added to the cells and RNAs were prepared from 0 to 4 hours thereafter. The level of VEGFC was determined by qPCR and was normalized to 36B4 mRNA. The relative amounts of VEGFC mRNA at time 0 before DRB addition were set to 100%.

### siRNA assay

siRNA transfection was performed using Lipofectamine RNAiMAX (Invitrogen). Cells were transfected with either 50 nmol/L of si-HuR (Ambion, 4390824, s4610) or si-Control (Ambion, 4390843). After 48 hours, cells were stimulated with 5 μmol/L of sunitinib or 5 μmol/L of sorafenib. Two days later, qPCR was performed, as described above.

### Gene expression microarray analysis

Normalized RNA sequencing data produced by The Cancer Genome Atlas (TCGA) were downloaded from cBiopotal (www.cbioportal.org, TCGA Provisional; RNA-Seq V2). Data were available for 503 of the 536 RCC tumor samples TCGA subjected to mRNA expression profiling. The subtype classifications were obtained through cBioPortal for Cancer Genomics and the 33 samples lacking classifications were discarded. The nonmetastatic group contained 424 patients and the metastatic group contained 79 patients. The results published here are in whole or in part based upon data generated by the TCGA

Research Network: http://cancergenome.nih.gov/ (27, 28). The Kaplan–Meier method was used to produce overall survival curves. The VEGFC z-score cut-off point for the overall survival was determined with the spline analysis. The effect of VEGFC and its OR was estimated using a Cox model adjusted to the expression of other genes and important patient characteristics.

### Patients and association studies

This was a retrospective study with all patients (312) consulted for a renal mass between 2008 and 2015 in Centre Antoine Lacassagne (Nice, France). Of these 312 patients, 87 only had been analyzed (cause of elimination of analyzable patients; no follow-up, renal metastasis from another cancer, RCC treated by surgery without metastasis, patients without progression . . .). The 87 patients had metastatic RCC treated in the first line with therapies including IFNα ± bevacizumab, sunitinib, temsirolimus. Only the patients that relapsed and patients without lymph node metastases before the treatment were included to test for the presence of lymph node metastases and new sites of metastasis on treatment [20 patients treated with sunitinib and 11 patients treated with other drugs (essentially with IFNα ± bevacizumab)]. Lymph node metastases and new sites of metastasis are two independent factors in comparison to age, gender, and metastatic stage at diagnostic (M0 or M1). Neoadjuvant patient samples were obtained from Nice, Bordeaux, and Monaco Hospitals. Patients were treated for at least two months before surgery (Supplementary Table S1A).

### Statistical analysis

***For in vitro and in vivo analysis.*** All data are expressed as the mean ± SEM. Statistical significance and *P* values were determined by the two-tailed Student *t* test. One-way ANOVA was used for statistical comparisons. Data were analyzed with Prism 5.0b (GraphPad Software) by one-way ANOVA with Bonferroni *post hoc*.

***For patient analysis.*** All categorical data were described using frequencies and percentages. Quantitative data were presented using median and range or mean and SD. Censored data were described using Kaplan–Meier estimation median survival and 95% confidence interval (CI). Statistical analyses were two sided and were considered to be significant if $P \leq 0.05$ using R 3.2.2.

***Univariate analysis.*** Statistical comparisons were made using $\chi^2$ test or Fisher exact test for categorical data, *t* test, or Wilcoxon test for quantitative data and log-rank test for censored data. Smoothing spline curves were used to predict death risk versus VEGFC mRNA expression.

***Multivariate analysis.*** Multivariate analysis was carried out by creating a Cox model. Choice of the final model was made performing backward stepwise model selection. All variables associated with $P \leq 0.1$ on univariate analysis were included in the model.

## Results

### Sunitinib stimulates VEGFC expression

To examine the relationship between tumor growth potential and VEGFC production, we used established and primary patient RCC cell lines that we developed in collaboration with the surgery department of the Nice Hospital (Nice, France; ref. 23) and stratified by aggressiveness. This was determined by (i) the ability to form tumors in mice (for established cell lines) and (ii) the time of overall survival of patients (for primary tumor cells). We observed that increases in aggressiveness corresponded to higher levels of VEGFC mRNA (Fig. 1A) and VEGFC production (Fig. 1B) in cell lines and primary cells. The reported intratumor concentrations of sunitinib in mice and patients were 5.5–13 μmol/L (29, 30). According to these results, we specifically used this range of concentrations in our experiments. Sunitinib induced an increase in the VEGFC mRNA level in six RCC cell lines (Fig. 1C) and in four primary tumor cells (Fig. 1D), while it did not change VEGFC mRNA in normal primary renal cells derived from three independent patients (Fig. 1E). Sunitinib increased VEGFC protein in the conditioned medium in the six RCC cell lines (Fig. 1F) and in the four independent primary cells (Fig. 1G) while it had no effect on normal cells (Fig. 1H). Our results show sunitinib-induced effects are transient as VEGFC mRNA amounts return to their basal levels following treatment cessation (Supplementary Fig. S1A). RCC cells do not express VEGFR1/2/3 (qPCR $\Delta C_t > 35$) but highly express CSF1R ($\Delta C_t$ 29), PDGFR ($\Delta C_t$ 22) and c-Kit ($\Delta C_t$ 25). Hence, aberrant expression of these receptors on tumor cells that was already reported (31–33) may explain the observed increase in VEGFC expression following sunitinib exposure. Moreover, we examined imatinib, a well-known inhibitor of c-Kit and PDGFR (like sunitinib), could similarly stimulate VEGFC expression (Supplementary Fig. S1B). Other VEGFR TKIs (i.e., axitinib, pazopanib, sorafenib) were also found to increase VEGFC mRNA in 786-O cells while bevacizumab/IFNα and the mTOR inhibitor everolimus did not (Supplementary Fig. S1C). Sorafenib, used as second-line therapy in RCC, upregulated VEGFC mRNA and protein levels in both established and primary tumor cells but had no effect on normal renal epithelial cells (Supplementary Fig. S1D to S1I). In cells adapted to a high concentration of sunitinib (10 μmol/L; Supplementary Fig. S2A and S2B; ref. 34), basal VEGFC mRNA and protein amounts were increased compared to naïve cells (Supplementary Fig. S2C and S2D). These results suggest a general mechanism by which drugs that directly or indirectly target angiogenesis induce VEGFC expression by tumor cells.

### Sunitinib stimulates VEGFC promoter activity

Sunitinib-mediated induction of VEGFC mRNA suggested stimulation of transcription, stabilization of mRNA, or a combination of both mechanisms. Hence, we first investigated the activity of the VEGFC promoter after sunitinib treatment. Sunitinib stimulated the activity of the VEGFC promoter in RCC cell lines (Fig. 2A) and in primary tumor cells (Fig. 2B). The transcription factor *sine oculis 1* (SIX1) participates in VEGFC transcription (15). We generated two reporter constructs, one with a VEGFC promoter containing SIX1-binding sites (long form) and one deleted of the SIX1 consensus site (short form, Fig. 2C). The long form was stimulated by sunitinib, while the short one was not, in four independent cell lines (Fig. 2D) and two primary tumor cells (Fig. 2E). VEGFC promoter activity was also higher in sunitinib-resistant cells (Supplementary Fig. S2F) generated previously by chronic exposure to the drug (34). As suggested by the increase in the mRNA levels (Supplementary Fig. S1C), sorafenib also stimulated activity of the VEGFC promoter in cell lines and primary cells (Supplementary Fig. S3A and S3B). These results

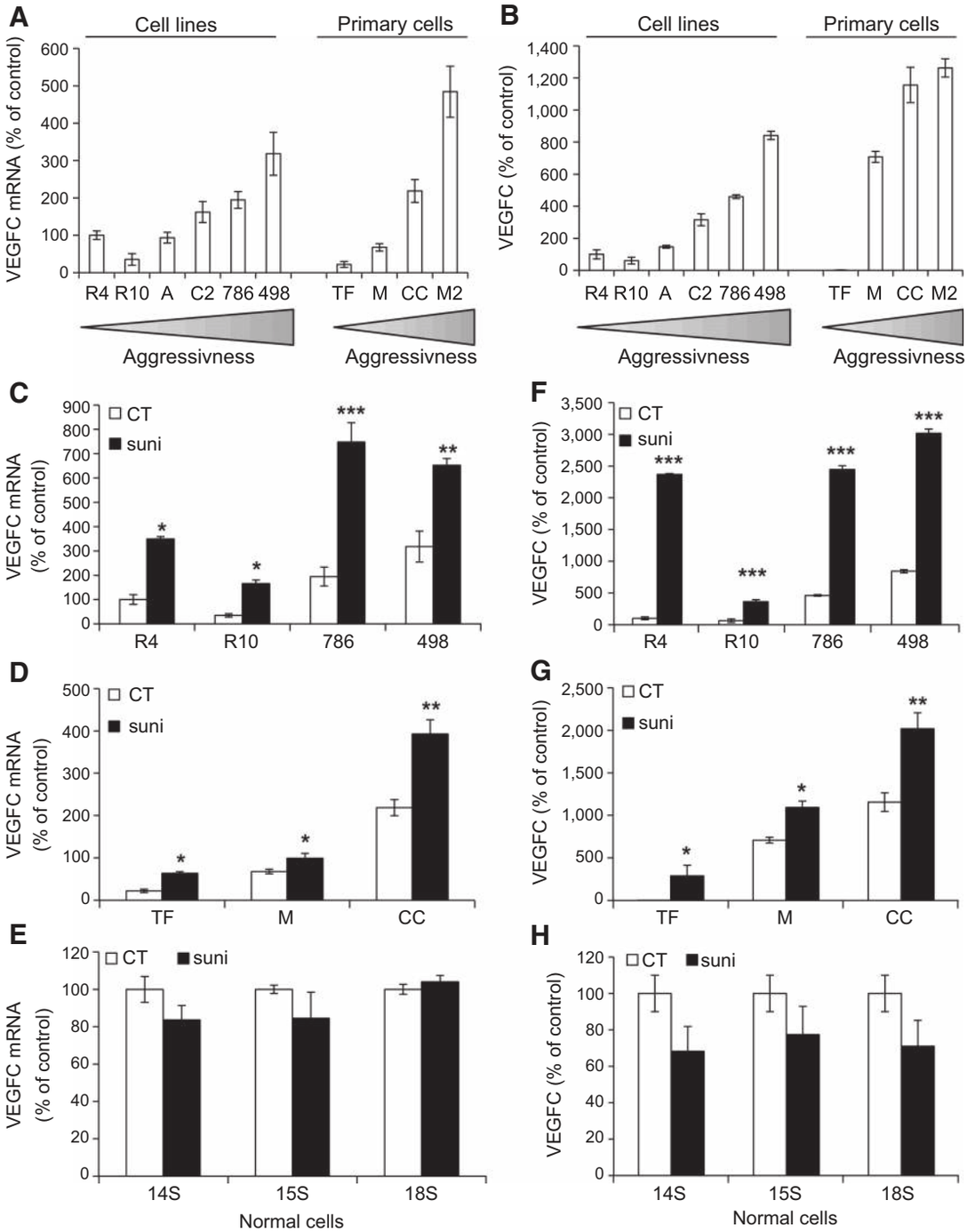


**Figure 1.**

Sunitinib increased VEGFC expression. **A–H,** Different RCC cell lines [RCC4 (R4), RCC10 (R10), ACHN (A), Caki-2 (C2), 786-O (786) and A498 (498)] and primary RCC cells (TF, M, CC, and M2) and normal renal cells (14S, 15S, and 18S) were evaluated for VEGFC mRNA levels by qPCR (**A, C, D, E**) and for VEGFC protein in cell supernatants by ELISA (**B, F, G, H**). **C** and **F,** RCC cell lines were treated with 5 μmol/L sunitinib (suni) for 48 hours. **D** and **G,** Primary cells were treated with sunitinib (10 μmol/L for TF, and 5 μmol/L for M and CC) for 48 hours. **E** and **H,** Normal kidney cells were treated with 5 μmol/L sunitinib for 48 hours. For **A**, **C**, and **D**, the mRNA level of R4 is considered as the reference value (100%). Data are represented as mean of three independent experiments ± SEM. *, $P < 0.05$; **, $P < 0.01$; ***, $P < 0.001$.

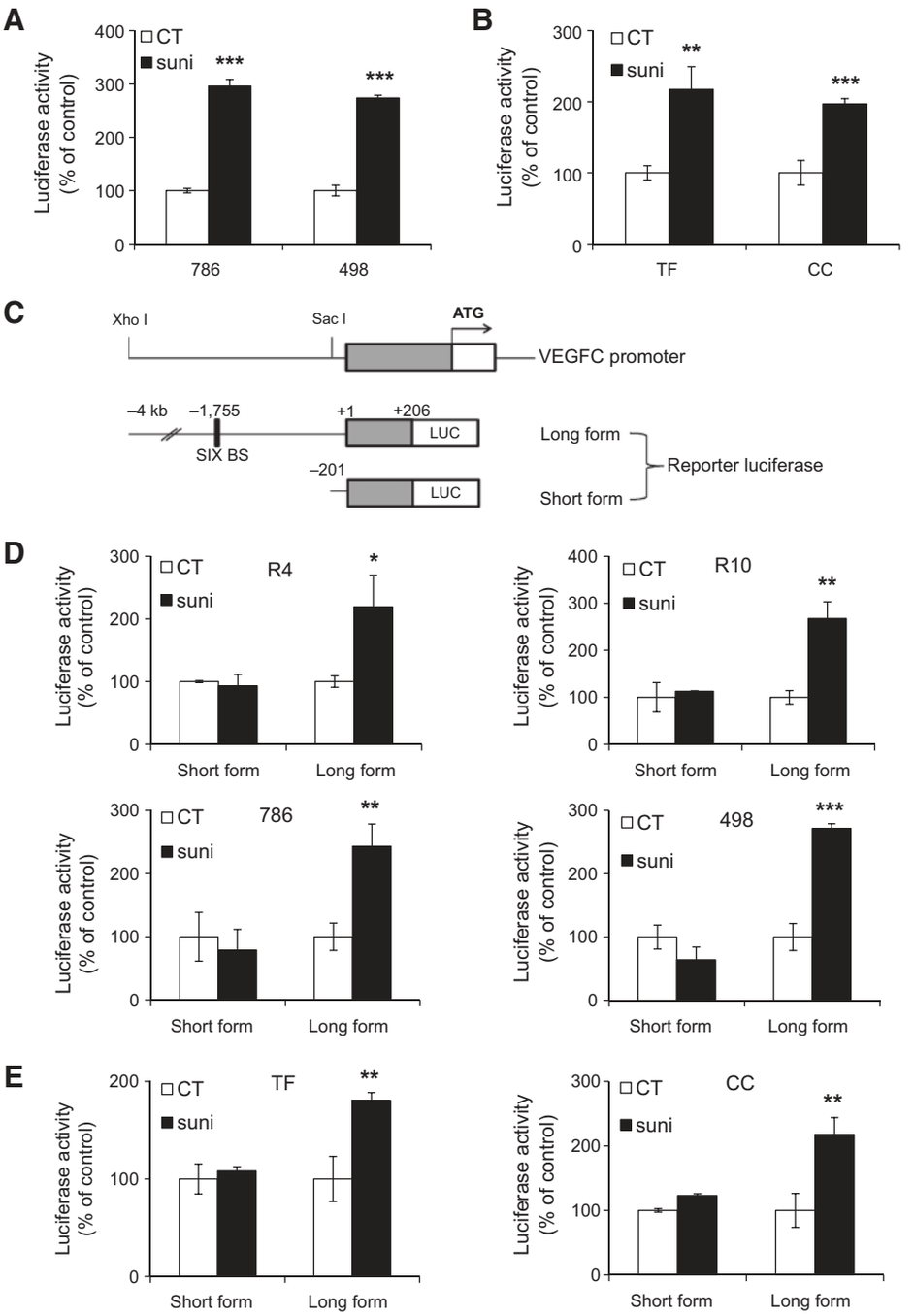


**Figure 2.**
Sunitinib increased VEGFC promoter activity. **A** and **B,** RCC cell lines (**A**) and primary cells (**B**) were transfected with a *Renilla* luciferase reporter gene under the control of the VEGFC promoter and treated with sunitinib (suni) 2.5 μmol/L for cell lines or 5 μmol/L for primary cells for 24 hours. The *Renilla* luciferase activity normalized to the firefly luciferase (control vector) was the readout of the VEGFC promoter activity. **C,** Schemas of truncated short and long forms of VEGFC promoter activity reporter genes used in **D** and **E**. **D** and **E,** RCC cell lines (**D**) and primary cells (**E**) were transfected with a firefly luciferase reporter gene under the control of the truncated short or long form VEGFC promoter and treated with sunitinib 2.5 μmol/L for cell lines or 5 μmol/L for primary cells for 24 hours. Normalized luciferase activity (control vector) was the readout of the VEGFC promoter activity. Data are represented as mean of three independent experiments ± SEM. *, $P < 0.05$; **, $P < 0.01$; ***, $P < 0.001$.

indicate transcriptional-dependent induction of VEGFC expression by antiangiogenic treatments.

### Sunitinib induces a 3′UTR-dependent increases in the VEGFC mRNA half-life

A second mechanism that may explain treatment-induced VEGFC mRNA increases is the stabilization of VEGFC mRNA. Indeed, sunitinib increased VEGFC mRNA half-life 6-fold in RCC cell lines (4.4 ± 2.8 hours vs. 26.5 ± 12.9 hours; Fig. 3A) and by 4-fold in primary cells (4.1 ± 3.9 hours vs. 16.7 ± 6.3 hours; Fig. 3B). Sorafenib also increased the VEGFC mRNA half-life (4.4 ± 2.8 hours vs. 14.8 ± 5.6 hours; Supplementary Fig. S3C). A reporter gene in which the VEGFC-3′UTR was inserted downstream of the luciferase gene (Fig. 3C) was also induced by sunitinib in two cell lines (Fig. 3D), two primary tumor cells (Fig. 3E), and in sunitinib-resistant cells (Supplementary Fig. S2G). Similarly, sorafenib stimulated the activity of the VEGFC-3′UTR reporter gene in both established and primary tumor cells (Supplementary Fig. S3D and S3E). These results demonstrate that two antiangiogenic treatments enhance VEGFC expression through the stabilization

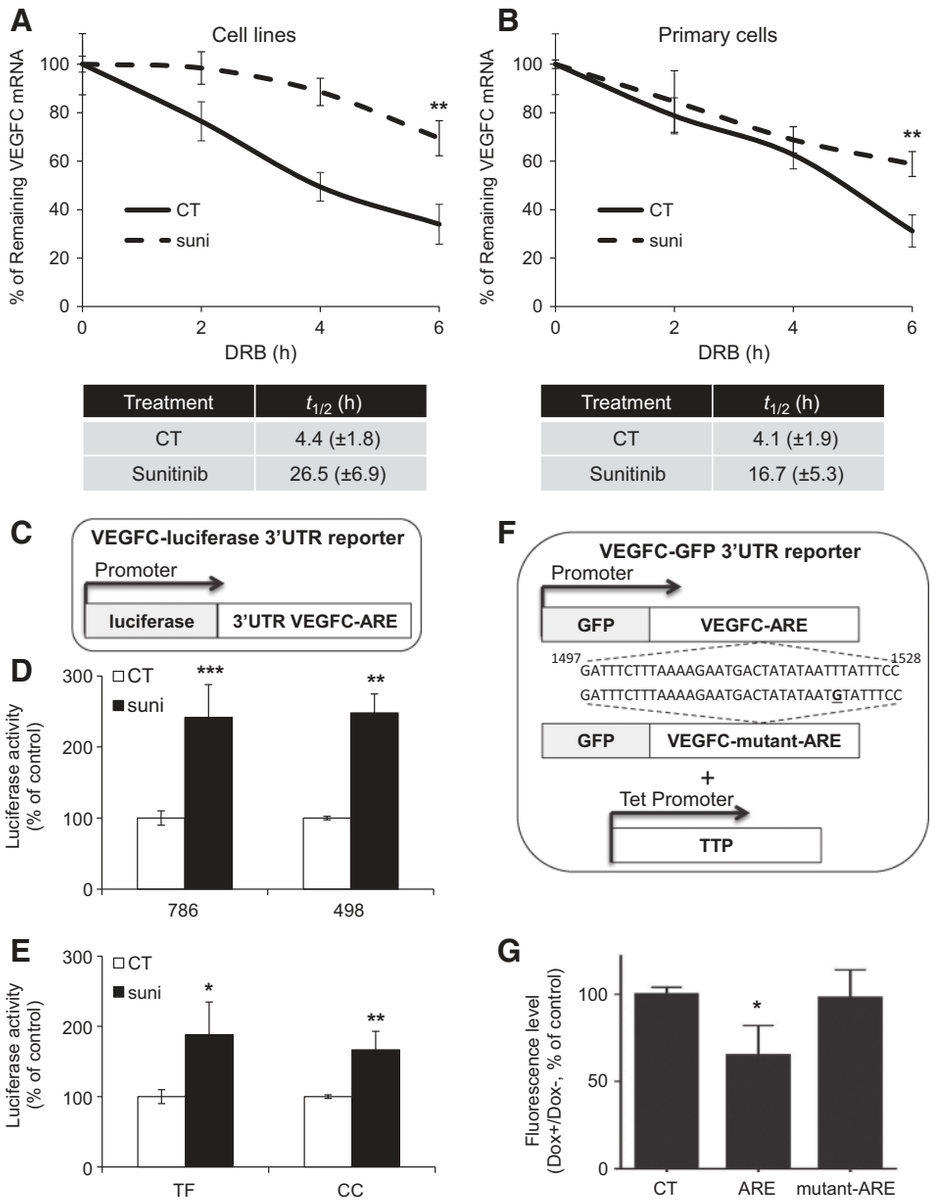


| Treatment | $t_{1/2}$ (h) |
|---|---|
| CT | 4.4 (±1.8) |
| Sunitinib | 26.5 (±6.9) |

| Treatment | $t_{1/2}$ (h) |
|---|---|
| CT | 4.1 (±1.9) |
| Sunitinib | 16.7 (±5.3) |

**Figure 3.**
Sunitinib increased the half-life of VEGFC mRNA via its 3′UTR. **A** and **B,** The RCC cell line (786-O; **A**) or primary cells (CC; **B**) were treated with 5 μmol/L sunitinib (suni) for 48 hours. Cells were then incubated with DRB for 2, 4, or 6 hours. The remaining VEGFC mRNA was evaluated by qPCR and its mRNA half-life was calculated. **C,** Schema of the VEGFC luciferase 3′UTR reporter gene. **D** and **E,** RCC cell lines (**D**) or primary cells (**E**) were transfected with the VEGFC 3′UTR reporter gene and treated with sunitinib 5 μmol/L (or 10 μmol/L for TF) for 24 hours. The normalized luciferase activity was the readout of the reporter gene mRNA half-life. **F,** Schemas of VEGFC GFP 3′UTR wild-type or mutated for the ARE element reporter genes. **G,** Cells were transfected with the VEGFC GFP 3′UTR wild-type or mutated reporter vectors for the VEGFC 3′UTR ARE. TTP expression was induced with 0.25 μg/mL doxycycline (dox). The fluorescence level was the readout of the reporter gene half-life. Data are represented as mean of three independent experiments ± SEM. *, $P < 0.05$; **, $P < 0.01$; ***, $P < 0.001$.

of its mRNA and via its 3′UTR. As for VEGFA, the VEGFC mRNA 3′UTR contains an adenylate and uridylate-rich element (ARE), a binding site for HuR and TTP. We used a wild-type or a VEGFC 3′UTR mutated for the ARE site coupled to the EGFP reporter gene (Fig. 3F). Expression of TTP, using a doxycycline-regulated construct, decreased the level of fluorescence only when the ARE site was present (Fig. 3G). These results suggest that TTP decreases VEGFC mRNA half-life by binding to its ARE in the 3′UTR.

### TTP and HuR bind VEGFC mRNA and modulate its half-life

Using RNA immunoprecipitation with antibodies to tagged-HuR and tagged-TTP, we found that HuR and TTP bound directly to VEGFC mRNA (Fig. 4A and B). TNFα and VEGFA mRNA binding served as positive controls and GFP and GAPDH mRNA as negative controls (Fig. 4A and B and Supplementary Fig. S3F and S3G). The balance between TTP and HuR activity determined the relative level of the target mRNA half-life (Fig. 4C). The phosphorylation of HuR stimulated its ability to stabilize a given mRNA, while phosphorylation of TTP played an opposite role (35). The expression of TTP is concomitant with a modification in molecular weight from a 36 kDa form (the form with maximal mRNA-destabilizing activity, only observed in LPS-stimulated RAW cells), to intermediate forms and finally to a low-mobility form of approximately 45 kDa. These different modifications highly depend on p38-dependent phosphorylation (36). While in nonstimulated 786-O cells, high-mobility and intermediate forms of TTP are present, sunitinib stimulation results in the accumulation of low-mobility forms corresponding to the maximally phosphorylated protein with impaired mRNA-destabilizing activity (37). HuR is not expressed in unstimulated or LPS-stimulated RAW cells. However, sunitinib stimulated HuR expression and the accumulation of its low-mobility/active forms

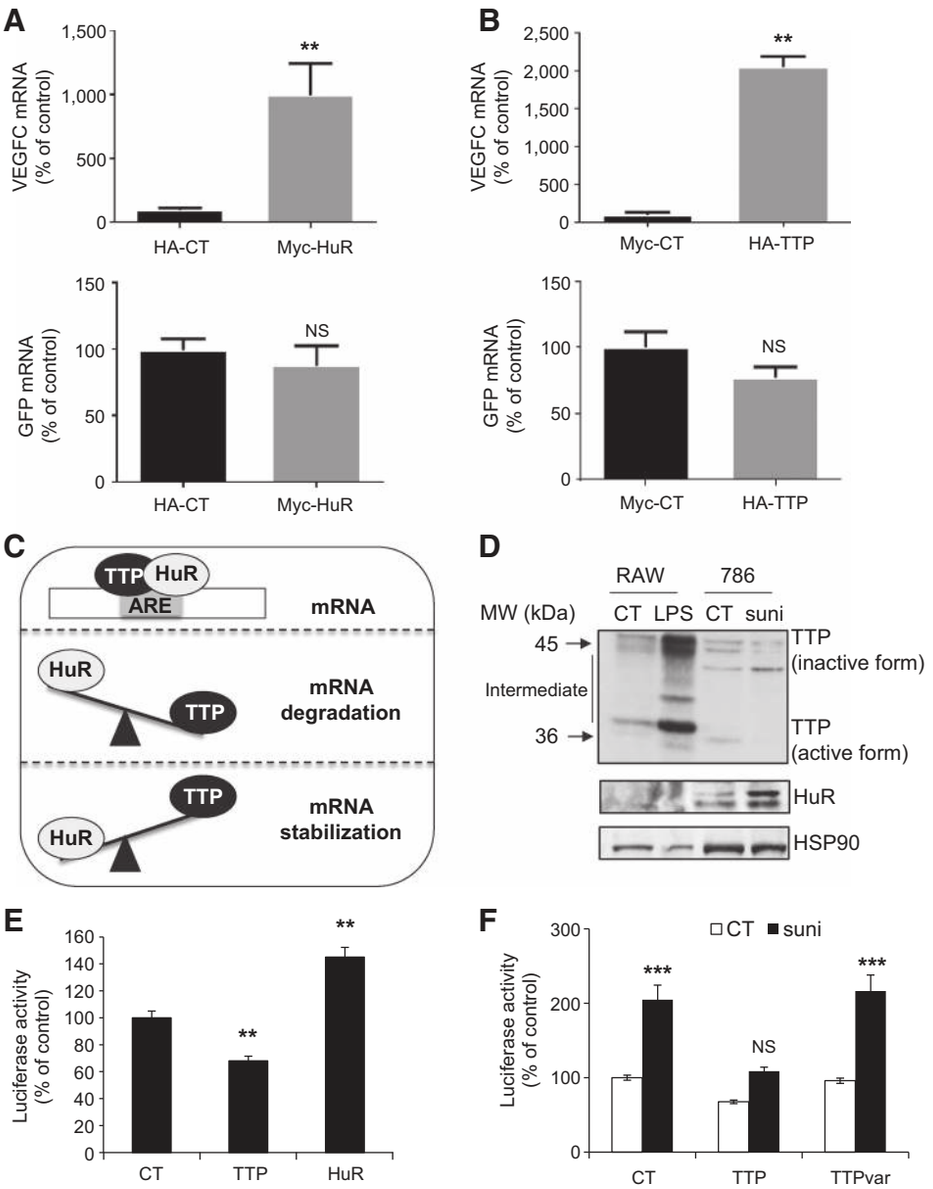


**Figure 4.**

TTP and HuR bind VEGFC mRNA and modulate its half-life. **A** and **B,** HuR/TTP interactions with VEGFC mRNA were analyzed by RIP-Chip (RNA-IP). HEK-293 cells were transfected with Myc-HuR or HA-CT (used as a negative control; **A**) or with HA-TTP and Myc-CT (used as a negative control; **B**). Exogenous TTP and HuR crosslinked to mRNA were immunoprecipitated with anti-HA and anti-Myc antibodies. The levels of immunoprecipitated VEGFC or GFP mRNA (used as a negative control) were assessed by qPCR. **C,** Schematic balance between TTP and HuR, and its effect on mRNA stability. **D,** RAW cells were stimulated with 10 μmol/L lipopolysaccharide (LPS) for 6 hours and were used as a positive control for active (unphosphorylated) and inactive [partially (intermediate) and fully phosphorylated form] forms of TTP. 786-O cells were stimulated with 5 μmol/L sunitinib (suni) for 6 hours. TTP and HuR expression was analyzed by Western blot analysis. HSP90 served as a loading control. **E** and **F,** 786-O cells were transfected with a VEGFC luciferase 3′UTR reporter gene in the presence of expression vectors for HuR, TTP, or TTPvar (a mutation that induces a decrease in TTP mRNA translation and serves as a negative control; ref. 38) and treated or not with sunitinib 5 μmol/L for 24 hours. The normalized luciferase counts served as readout of the reporter gene mRNA half-life. Data are represented as mean of three independent experiments ± SEM. **, $P < 0.01$; ***, $P < 0.001$. NS, nonsignificant.

(Fig. 4D). Overexpression of TTP decreased VEGFC 3′UTR reporter activity while overexpression of HuR increased it (Fig. 4E). Moreover, overexpression of TTP inhibited the sunitinib-dependent increase in the VEGFC 3′UTR reporter activity while overexpression of a mutated form of TTP that is poorly translated (TTPvar; ref. 38) did not (Fig. 4F). These results suggest that a regulated balance of active TTP and HuR plays a key role in the regulation of the VEGFC mRNA half-life induced by sunitinib.

### p38 and HuR are required for sunitinib-dependent increases in VEGFC expression

ERK and p38 pathways are critical for the modulation of the TTP and HuR activity (39). Sunitinib induced rapid activation of the ERK and p38 pathways determined by the presence of their phosphorylated forms (p-ERK and p-p38). Activation of ERK and p38 correlated with an increase in HuR amounts and to its cytoplasmic translocation (active forms) in established RCC cell lines (Fig. 5A; Supplementary Fig. S4A) and in primary tumor cells (Supplementary Fig. S4B). Inhibition of ERK (PD184352) did not modify the sunitinib-dependent increase of the VEGFC mRNA, while inhibition of p38 (SB203580) strongly reduced it in an established cell line (Fig. 5B; Supplementary Fig. S4C) and in primary tumor cells (Supplementary Fig. S4D). Phospho-p38 basal activity increased in sunitinib-resistant cells and was correlated with enhanced VEGFC expression (Supplementary Fig. S2C–S2E). Inhibition of p38 reduced the sunitinib-dependent increase in the VEGFC mRNA half-life and the VEGFC 3′UTR reporter gene activity in an established RCC cell line (Fig. 5C and D) and in primary tumor cells (Supplementary Fig. S4E). Moreover, SB203580 inhibited the sunitinib-dependent induction of HuR (Fig. 4E). These results suggested that VEGFC upregulation of the mRNA half-life is

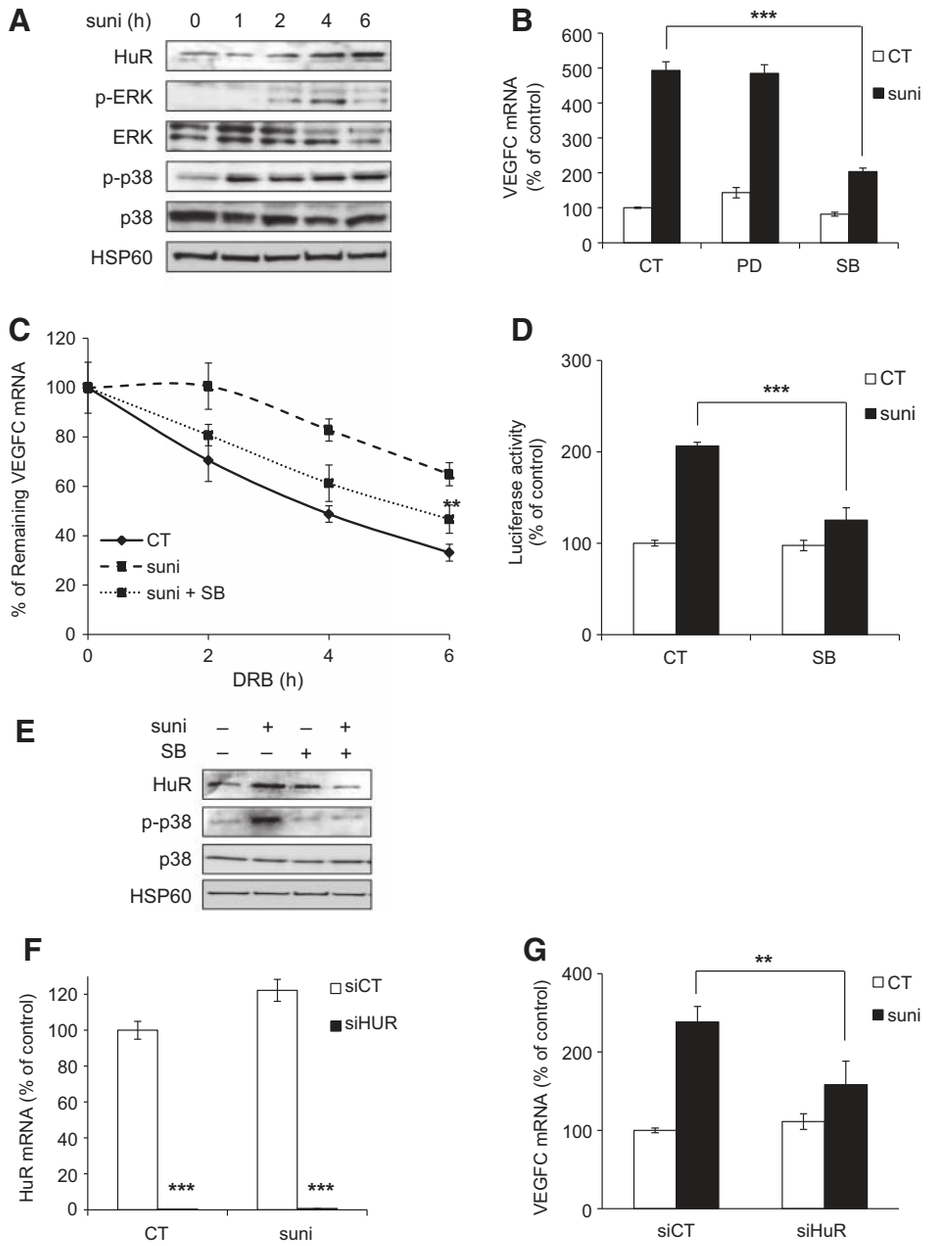


**Figure 5.**
p38 and HuR were required for the induction of VEGFC expression by sunitinib. **A,** 786-O cells were treated with 5 μmol/L sunitinib (suni) for 1 to 6 hours. HuR, p-ERK, ERK, p-p38, and p38 expression was analyzed by immunoblotting. HSP60 served as a loading control. **B,** 786-O cells were treated with 5 μmol/L sunitinib in the presence of 10 μmol/L PD184352 (PD, ERK inhibitor) or 10 μmol/L SB203580 (SB, p38 inhibitor) for 48 hours. The VEGFC mRNA level was determined by qPCR. **C,** 786-O cells were treated with 5 μmol/L sunitinib with or without 10 μmol/L SB203580 for 48 hours. Cells were then treated with DRB for 2, 4, or 6 hours. The remaining VEGFC mRNA was evaluated by qPCR. **D,** 786-O cells were transfected with a VEGFC luciferase 3′UTR reporter gene and treated or not with 5 μmol/L sunitinib and/or with 10 μmol/L SB203580 for 24 hours. The normalized luciferase counts served as a readout of the reporter gene mRNA half-life. **E,** 786-O cells were treated with 5 μmol/L sunitinib and/or 10 μmol/L SB203580. HuR, p-p38, and p38 expression was analyzed by immunoblotting. HSP60 served as a loading control. **F** and **G,** 786-O cells were transfected with CT or HuR siRNA. Twenty-four hours later, cells were treated with 5 μmol/L sunitinib for 48 hours. HuR (**F**) and VEGFC (**G**) mRNA levels were determined by qPCR. Data are represented as mean of three independent experiments ± SEM. **, $P < 0.01$; ***, $P < 0.001$.

dependent on HuR induction via stimulation of the p38 pathway. Hence, downregulation of HuR with siRNA inhibited the sunitinib-dependent increase of VEGFC mRNA in a RCC cell line (Fig. 5F and G) and in primary tumor cells (Supplementary Fig. S4F and S4G). These results confirmed that sunitinib induces a cascade of events starting from early activation of p38 to activation of HuR that finally results in induction of VEGFC mRNA expression.

### Sunitinib induces lymphangiogenesis *in vivo*

To correlate the sunitinib-dependent induction of VEGFC expression to lymphangiogenesis, we evaluated the presence of lymphatic vessels in experimental RCC tumors obtained by subcutaneous injection of 786-O cells in nude mice. Mice were treated with sunitinib after the tumors reached 100 $mm^3$ for approximately one month before analysis. Sunitinib stimulated lymphangiogenesis was confirmed by the presence of LYVE1-positive lymphatic endothelial cells (LEC) in the core of the implanted tumors after treatment while no staining was observed in the core of control tumors (Fig. 6A and B). Phospho-p38 labeling was also increased in tumors of sunitinib-treated mice, which confirmed *in vitro* observations (Fig. 6C and D). The levels of human (produced by xenotransplanted tumor cells) and mouse (stromal cells) VEGFC and HuR mRNA were increased in the tumors of mice treated with sunitinib in comparison with the levels of both factors in the tumors of nontreated mice (Supplementary Fig. S5A). Sunitinib also induced the expression of genes involved in lymphangiogenesis

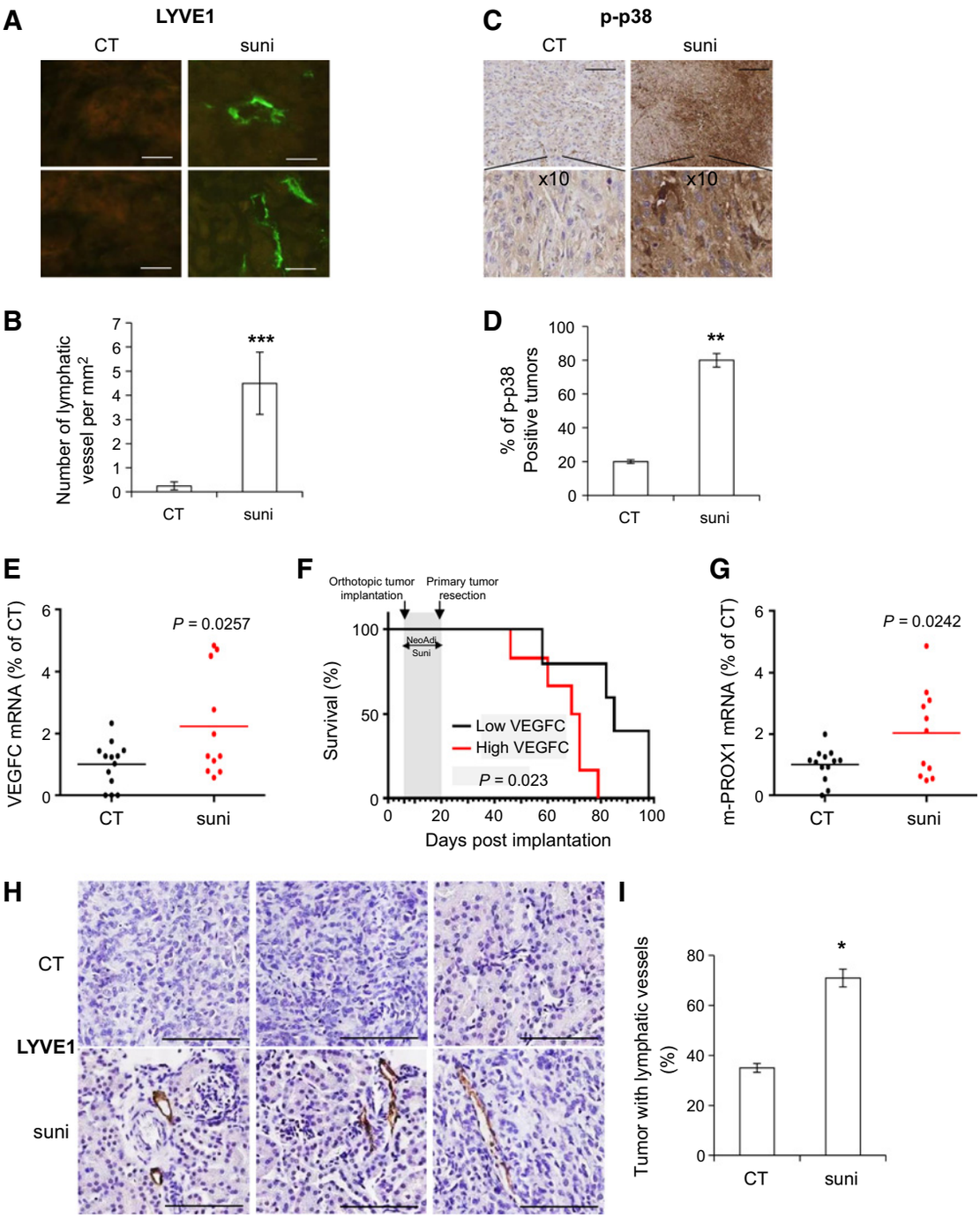


**Figure 6.**

Sunitinib induced lymphangiogenesis *in vivo*. **A–E,** Experimental tumors obtained after subcutaneous injection of $5 \times 10^6$ 786-O cells were analyzed for LYVE1 expression. **A,** Lymphatic endothelial cells were detected by LYVE1 immunolabeling (green). Scale bar, 20 μm. **B,** Quantification of the LYVE1-positive vessels per $mm^2$ ($n = 20$). **C,** p-p38 was detected by IHC. Scale bar, 20 μm. **D,** Quantification of p-p38–labeled cells ($n = 20$). **E–I,** $SN12PM6^{LUC+}$ ($2 \times 10^6$ cells) were implanted into the kidney (subcapsular space) of 6 to 8-week-old female CB17 SCID. **E,** VEGFC mRNA mRNA levels in tumors from control mice and mice treated in a neoadjuvant setting ($n = 24$). **F,** The Kaplan–Meier analysis of mice treated or not with sunitinib and the prognostic role of VEGFC mRNA levels ($n = 24$). **G,** PROX1 mRNA levels in tumors from control mice and mice treated in a neoadjuvant setting ($n = 24$). **H,** Lymphatic endothelial cells were detected by LYVE1 IHC. Scale bar, 20 μm. **I,** Quantification of the LYVE1-positive vessels ($n = 24$). *, $P < 0.05$; **, $P < 0.01$; ***, $P < 0.001$.

including *vegfr3*, *nrp2*, *prox1* by cells of the microenvironment (mouse; Supplementary Fig. S5A). Increased expression of proangiogenic genes upon sunitinib treatment (*vegfa*, *vegfr1*, *nrp1*, *and α-sma*) was observed (Supplementary Fig. S5A) but blood vessel maturation attested by coverage of endothelial cells (CD31 labeling) by pericytes (α-SMA labeling) was equivalent in control or sunitinib-treated mice tumors (Supplementary Fig. S5B). Together, these results suggest that sunitinib did not alter the vascular network function but induced lymphatic network development, potentially increasing tumor metastatic potential. To examine this, we performed a retrospective analysis of lymphatic marker expression in human RCC cells (SN12-PM6$^{LUC+}$) implanted orthotopically in SCID mice, treated neoadjuvantly with sunitinib, and then surgically resected as described by Ebos and colleagues (24). In these studies, neoadjuvant sunitinib treatment was found to have no benefit in reducing primary tumor growth but, following surgery and sunitinib treatment withdrawal, increased metastasis and reduced overall survival. Our results show VEGFC level increases in excised tumors from sunitinib-treated mice (Fig. 6E) and a majority of mice that were treated in a neoadjuvant setting developed metastasis as shown previously (24). Strikingly, high VEGFC levels in tumors from sunitinib-treated mice were correlated with shorter survival (Fig. 6F). This observation is consistent with the development of a lymphatic network shown by the increases in PROX1 levels (Fig. 6G) and the presence of LYVE1-positive lymphatic vessels (35% in control mice vs. 70% in sunitinib-treated mice; Fig. 6H and I). Together, these results suggest a strong correlation between sunitinib treatment and a VEGFC/lymphatic vessel–dependent, which may, in turn, impact metastatic progression and reduce survival.

**Sunitinib is associated with increased lymphangiogenesis and lymph node metastasis in RCC patients**

There are several benefits to neoadjuvant treatment including (i) the downsizing of renal tumors to facilitate surgery or ablative approaches (which can preserve renal function), (ii) to assess patient sensitivity to treatment (if recurrence occurs), and (iii) to prevent metastatic spread (thereby improving post-surgical survival; ref. 40). However, the benefits of neoadjuvant antiangiogenic treatments have yet to be validated clinically (40), thus examination of patient materials is rarely performed. However, we obtained 13 patient samples (from a total of 3,000) that were treated with antiangiogenic therapy in a neoadjuvant setting in different French hospitals (Supplementary Table S1A). Treated tumor samples were compared with tumors of untreated patients for the presence of lymphatic vessels. While lymphatic vessels were detected in 4 of 20 tumors (20%) from untreated patients, we found that lymphatic vessels in 9 of 13 tumors (69.2%, $P = 0.005$) from patients treated in a neoadjuvant setting (Fig. 7A and B). The presence of lymphatic vessels correlated with an increase in VEGFR3, NRP2, PROX1, LYVE1, and HuR mRNA levels (Fig. 7C). VEGFC levels (Fig. 7C) and p-p38 were not modified, which we speculate to be due to sunitinib treatment that was stopped for more than one month before surgical resection to allow wound-healing processes. This result was consistent with the transient effect of sunitinib of VEGFC expression that we observed *in vitro* (Supplementary Fig. S1A). Sunitinib in a neoadjuvant setting was not associated with tumor blood vascular changes (CD31 and α-SMA labeling; Supplementary Fig. S6C and S6D). We next compared the presence of lymph node metastasis in nonresponder patients treated with sunitinib (20 of 87 patients with metastatic RCC; see Methods) or other therapeutic options including IFNα, bevacizumab, and a mTOR inhibitor (temsirolimus, 11 of 87 patients; Supplementary Table S1B).

Thirty-five percent (7/20) of patients treated with sunitinib developed lymph node metastasis and new metastatic sites, whereas patients treated with other therapeutic options did not (0/11; $P = 0.033$; Fig. 7D). As expected, patients with lymph node invastion (N1) and new metastatic sites had a shorter overall survival ($P = 0.012$; Fig. 7D).

This result reinforces our conclusion that sunitinib stimulates the development of a lymphatic network. Finally, cBioPortal analysis showed that high amounts of VEGFC correlated with decreased overall survival ($P = 0.0026$; Supplementary Fig. S6A) and an increased proportion of metastatic patients ((M1 patients) $P = 0.019$; Supplementary Fig. S6B). The level of VEGFC, the tumor stage, the metastatic status (M1) and the lymph node invasion (N1) were analyzed in a multivariate Cox regression model on overall survival. VEGFC expression was identified as an independent prognostic parameter for overall survival ($P = 0.000253$; Supplementary Fig. S6C).

## Discussion

Resistance to antiangiogenic treatments are classified into: (i) intrinsic resistance; tumors fail to respond from the outset of treatment, (e.g., through sequestration of sunitinib in lysosomes; ref. 34), and (ii) acquired resistance; induction of compensatory pathways (41) including an increase in growth factor expression (e.g., Increased VEGFC and resulting lymphangiogenesis), as we have shown in this study. Eighty percent of metastases of solid cancers are estimated to disseminate through the lymphatic system, while 20% of metastases may occur through the blood vasculature or by direct seeding (12). Lymph node metastasis is the first sign of tumor progression in the majority of epithelial malignancies (12) (invasion of sentinel lymph nodes in breast cancers is directly linked to prognosis). An increased density of peri- and intratumor lymphatic vessels, as we observed in tumors from sunitinib-treated mice, indicates activation of lymphangiogenesis. A significant correlation has been observed between lymphatic vessel density and lymph node and organ metastasis in clinical studies. High expression levels of the lymphangiogenic factor VEGFC correlates with lymph node metastasis in numerous tumor types. Overexpression of VEGFC or VEGFD in mouse models increases the lymphatic vessel density and diameter of lymph nodes and organ metastasis (12). Intratumor lymphatic vessels and increased metastasis had been observed in VEGFC-overexpressing tumors implanted in mice (12). Furthermore, lymphatic invasion by RCC cells was the only independent risk factor for lymph node metastasis (42). Whereas sunitinib and sorafenib increased VEGFC transcription and mRNA stabilization, they did not increase VEGFD expression in our RCC model systems. Strikingly, VEGFD mRNA 3′UTR does not contain ARE. Sunitinib increased VEGFC expression only in tumor cells and not in normal cells (kidney cells and LEC), suggesting specific genetic particularities that mediate tumor cell adaptation to a toxic drug. Our results are consistent with those of Sennino and colleagues who described VEGFC

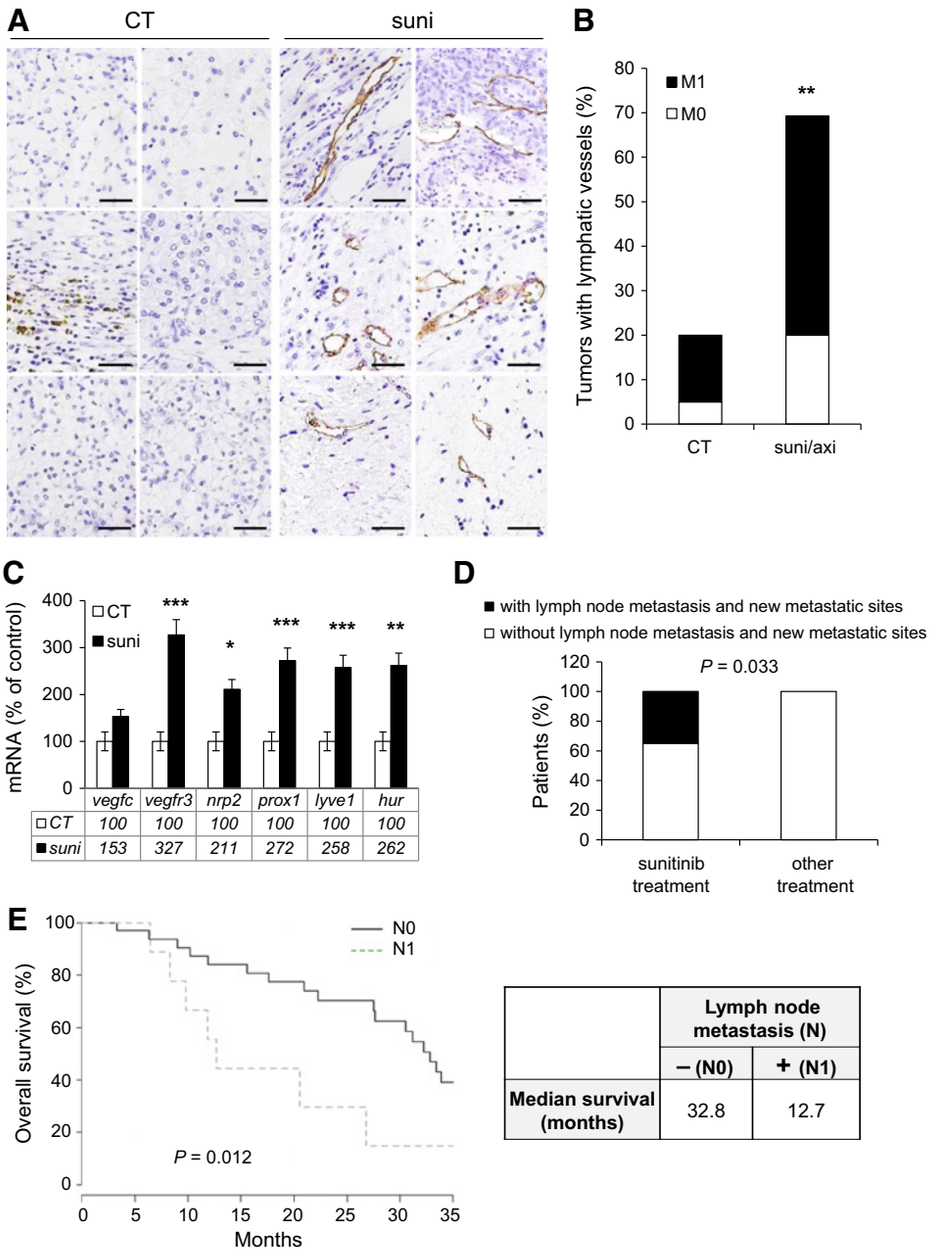


| | Lymph node metastasis (N) | |
|---|---|---|
| | − (N0) | + (N1) |
| Median survival (months) | 32.8 | 12.7 |

**Figure 7.**
Sunitinib induced lymphangiogenesis and metastasis in lymph nodes of RCC patients. Tumors from untreated RCC patients and tumors from patients treated with sunitinib or axitinib in a neoadjuvant setting were compared (see Supplementary Table S1A). **A,** Lymphatic endothelial cells were detected by podoplanin (PDN) immunolabeling (brown). Scale bar, 25 μm. **B,** Quantification of the podoplanine (PDN)-positive vessels. **C,** The levels of indicated mRNA were determined by qPCR. **D,** RCC patients that progressed on treatment were analyzed for the presence of lymph node metastasis and new metastatic sites (two or more new sites). Patients were stratified for sunitinib or other antiangiogenic treatments (see Supplementary Table S1B). **E,** The Kaplan–Meier analysis of patients that had relapsed on sunitinib with noninvaded or *de novo* invaded lymph nodes.

induction in response to antiangiogenic drugs in a mouse model of pancreatic tumors (43). Regorafenib, another multikinase TKI with similar targets as sunitinib, did not stimulate VEGFC expression. Unlike sunitinib, regorafenib inhibits p38 activity, reinforcing the specific role of p38 in the sunitinib-dependent increase of VEGFC expression. Unfortunately, this treatment has not been approved for clinical use because of its side effects (44). Regulation of VEGFC expression has been poorly addressed (45). *Vegfc* gene transcription depends on the transcription factor SIX1, which is overexpressed in metastatic breast cancers (15). The critical role for SIX1 in lymphatic dissemination of breast cancer cells provides a direct mechanistic explanation linking VEGFC expression, lymphangiogenesis, and metastasis (15). Sunitinib did not stimulate the VEGFC promoter deleted from the domain containing SIX1-binding sites, suggesting that it may play a role. However, the deleted domain also contains binding sites for NF-κB, GATA-2 and 3, Erg-1, and p53 transcription factors. Hence, further experiments are needed to determine the transcription factors implicated in the sunitinib-dependent stimulation of *vegfc* gene transcription. Analysis of available online databases (TGCA) with cBioPortal (http://www.cbioportal.org) showed that overexpression of SIX1 does not correlate with short progression-free or overall survival for patients with metastatic RCC unlike for breast cancers patients, whereas VEGFC is a factor correlated with poor prognosis, suggesting that SIX1 is not the major driver of *vegfc* gene transcription in these tumors. VEGFC expression is regulated at the level of its mRNA half-life by a

subtle balance between HuR and TTP. By increasing the half-life of a specific mRNA, HuR enhances the levels of proteins that promote cell proliferation, increase cell survival and local angiogenesis, help the cancer cells to evade immune recognition, and facilitate cancer cell invasion and metastasis (46). High levels of cytoplasmic HuR have been found in oral, colorectal, gastric, lung, breast, ovarian, renal, skin carcinomas, and mesothelioma. Stromal cells and adjacent nontumor tissues do not show cytoplasmic expression of HuR (47). Cytoplasmic HuR expression is associated with reduced RCC survival (48) and downregulation of HuR inhibits cell proliferation and induces apoptosis of RCC cells (49). Cytoplasmic expression of HuR is associated with lymph node metastasis and advanced disease in non–small cell lung, colon, and upper urinary tract urothelial carcinomas. The cytoplasmic levels of HuR are increased in tumors with lymphatic/vascular invasion compared with tumors without vessel invasion in cervical, colon, and *in situ* breast ductal carcinomas (47). These results are consistent with sunitinib-dependent activation of HuR, increased VEGFC mRNA half-life, and lymphangiogenesis. Sunitinib was shown to diminish the postsurgical benefits of neoadjuvant sunitinib treatment in mice, including the promotion of metastasis (and decrease in survival) of select RCC models. Initial observations suggested that sunitinib modified the localization of the metastases and could increase incidence in the lymphatic vessels of spleen and stomach, two organs drained to a large extent by lymphatic vessels (24). These findings are consistent with our results showing that sunitinib increased VEGFC expression and lymphangiogenesis. Sunitinib also induced VEGFR2 and VEGFR3 expression in LEC *in vitro* and in stromal cells *in vivo*. Expression may favor the paracrine action of VEGFC overexpressed by tumor cells after sunitinib treatment on LEC and the development of a lymphatic network in the tumor. Whereas sunitinib inhibits VEGFR2 and VEGFR3, the accumulation of VEGFC may act during the treatment break that is part of the sunitinib regimen (four weeks of treatment followed by a two week holiday to limit toxicity). Alternatively, VEGFC may stimulate neuropilin-2 (NRP2), the coreceptor of VEGFR3, which is overexpressed on RCC cells (50). The importance of NRP2 during the initiation of new lymphatic vessel sprouts was detected in hypoplastic lymphatic vessels observed in *nrp2* gene–targeted mice. Among other structures, NRP2 is expressed on veins and upregulated in tumor-associated lymphatic vessels where it binds VEGFC, VEGFA, and partially processed VEGFD (12). Moreover, blocking NRP2 function inhibits tumor cell metastasis (51). NRP2 expressed on cancer cells interacts with alpha 5 integrin on endothelial cells to mediate vascular extravasation and promotion of metastasis in zebrafish and murine xenograft models of RCC and pancreatic adenocarcinoma (50). Moreover, NRP2 correlates with poor prognosis in patients with advanced RCC. The median overall survival was longer for patients with low levels of NRP2 (26 months) compared with patients overexpressing NRP2 (13 months; ref. 52). NRP2 mRNA is increased in tumors of mice treated with sunitinib. For this reason, cotreatment with sunitinib and VEGFC-blocking agents may be a good option for RCC patients to reduce the progression of the disease. This cotreatment could result in the reduction of the sunitinib dose, avoiding intercure during which lymphatic vessels may develop.

Our study showed that sunitinib correlated to lymphatic invasion in experimental and human tumors. A quick appraisal of these results could be that sunitinib is detrimental for patients, which is absolutely not the case (Supplementary Table S1B; refs. 10, 11). Our results confirm that sunitinib compared with other treatments prolonged survival but suggest a fraction of the nonresponder patients had more invaded lymph nodes and new metastatic sites compared with nonresponder patients treated with other therapeutic agents, a potential reason for progression on treatment. Our results suggest that combining VEGFC inhibitors with sunitinib could limit the progression of the disease. In an analyzed cohort, 28% of patients stopped sunitinib treatment because of intolerance. New TKIs like axitinib or pazopanib are better tolerated or provide a better health-related quality of life (53). Moreover, they have an acidic pKa that prevents their sequestration in lysosomes, a mechanism associated with resistance to sunitinib (34). However, both inhibitors also target PDGFR and cKit and similarly stimulated VEGFC (Supplementary Fig. S1). This is another argument for the combination of TKI with VEGFC inhibitors. To conclude, overexpression of VEGFC represents an extrinsic mechanism of adaptation of RCC leading to drug resistance.

For multikinase TKIs such as sunitinib and sorafenib, VEGFC is induced in an VEGFR-independent manner even *in vitro*, but for VEGFR-selective TKIs, VEGFC is induced only *in vivo*, suggesting that in those cases the target cells are stromal. A recapitulated schema is shown in Supplementary Fig. S7. Although sunitinib has revolutionized the care of patients, its efficacy may be improved by targeting VEGFC-dependent development of the lymphatic network, a major route of spread of tumor cells when the patients become resistant to therapy.

## Disclosure of Potential Conflicts of Interest

No potential conflicts of interest were disclosed.

## Authors' Contributions

**Conception and design:** M. Dufies, S. Giuliano, K.S. Khabar, R. Grépin, G. Pagès
**Development of methodology:** M. Dufies, S. Giuliano, P.D. Ndiaye, E. Chamorey, J. Parola, J.M. Ferrero, G. Pagès
**Acquisition of data (provided animals, acquired and managed patients, provided facilities, etc.):** M. Dufies, D. Ambrosetti, A. Claren, L.S. Cooley, E. Chamorey, V. Vial, J.C. Bernhard, A. Ravaud, D. Borchiellini, J.M. Ferrero, R. Grépin, G. Pagès
**Analysis and interpretation of data (e.g., statistical analysis, biostatistics, computational analysis):** M. Dufies, S. Giuliano, D. Ambrosetti, M. Mastri, M. Ettaiche, E. Chamorey, J.M. Ferrero, J.M. Ebos, G. Pagès
**Writing, review, and/or revision of the manuscript:** M. Dufies, D. Ambrosetti, M. Lupu-Plesu, A. Ravaud, D. Borchiellini, J.M. Ferrero, A. Bikfalvi, J.M. Ebos, K.S. Khabar, G. Pagès
**Administrative, technical, or material support (i.e., reporting or organizing data, constructing databases):** W. Moghrabi, J. Parola, J.M. Ferrero, G. Pagès
**Study supervision:** R. Grépin, G. Pagès

## Acknowledgments

We thank Dr. Baharia Mograbi for help with cBioPortal analysis, Dr. Christiane Brahimi-Horn for editorial assistance, Dr. Ophélie Cassuto for help with analysis of patient records, and Maher Al-Saif for technical assistance in ARE cloning. We also thank Dr. Heide L. Ford and Dr. Kari Alitalo for the kind gift of VEGFC promoter reporter genes.

## Grant Support

This work was supported by the French association for cancer research (ARC; to G. Pagès), the French National Institute for Cancer Research (INCA; to G. Pagès), the Fondation de France (S. Giuliano and M. Dufies), the Fondation d'entreprise Groupe Pasteur Mutualité (M. Dufies), the Framework Program 7 of the European Commission –

Marie Curie Intra-European grant "VELYMPH" (M. Lupu-Plesu), the U.S. Department of Defense under Award no. W81XWH-14-1-0210 (J.M. Ebos), "Cordon de Vie" Monaco (S. Giuliano), and IRIS Pharma. The Bordeaux samples and associated data were collected, selected, and made available under the project clinicobiological National Cancer Database Kidney UroCCR supported by l'Institut National du Cancer (INCA; to A. Ravaud and J.-C. Bernhard).

The costs of publication of this article were defrayed in part by the payment of page charges. This article must therefore be hereby marked *advertisement* in accordance with 18 U.S.C. Section 1734 solely to indicate this fact.

Received November 15, 2016; revised December 7, 2016; accepted December 8, 2016; published OnlineFirst January 13, 2017.

## References

1. Eisen T, Sternberg CN, Robert C, Mulders P, Pyle L, Zbinden S, et al. Targeted therapies for renal cell carcinoma: review of adverse event management strategies. J Natl Cancer Inst 2012;104:93–113.
2. Escudier B. Sunitinib for the management of advanced renal cell carcinoma. Expert Rev Anticancer Ther 2010;10:305–17.
3. Giuliano S, Pages G. Mechanisms of resistance to anti-angiogenesis therapies. Biochimie 2013;95:1110–9.
4. Ribatti D. Tumor refractoriness to anti-VEGF therapy. Oncotarget 2016;7:46668–77.
5. Wang Z, Dabrosin C, Yin X, Fuster MM, Arreola A, Rathmell WK, et al. Broad targeting of angiogenesis for cancer prevention and therapy. Semin Cancer Biol 2015;35:S224–43.
6. Welti J, Loges S, Dimmeler S, Carmeliet P. Recent molecular discoveries in angiogenesis and antiangiogenic therapies in cancer. J Clin Invest 2013;123:3190–200.
7. Ebos JM, Lee CR, Cruz-Munoz W, Bjarnason GA, Christensen JG, Kerbel RS. Accelerated metastasis after short-term treatment with a potent inhibitor of tumor angiogenesis. Cancer Cell 2009;15:232–9.
8. Paez-Ribes M, Allen E, Hudock J, Takeda T, Okuyama H, Vinals F, et al. Antiangiogenic therapy elicits malignant progression of tumors to increased local invasion and distant metastasis. Cancer Cell 2009;15:220–31.
9. Ebos JM. Prodding the beast: assessing the impact of treatment-induced metastasis. Cancer Res 2015;75:3427–35.
10. Blagoev KB, Wilkerson J, Stein WD, Motzer RJ, Bates SE, Fojo AT. Sunitinib does not accelerate tumor growth in patients with metastatic renal cell carcinoma. Cell Rep 2013;3:277–81.
11. Miles D, Harbeck N, Escudier B, Hurwitz H, Saltz L, Van Cutsem E, et al. Disease course patterns after discontinuation of bevacizumab: pooled analysis of randomized phase III trials. J Clin Oncol 2011;29:83–8.
12. Alitalo A, Detmar M. Interaction of tumor cells and lymphatic vessels in cancer progression. Oncogene 2012;31:4499–508.
13. Tammela T, Zarkada G, Wallgard E, Murtomaki A, Suchting S, Wirzenius M, et al. Blocking VEGFR-3 suppresses angiogenic sprouting and vascular network formation. Nature 2008;454:656–60.
14. Su JL, Yen CJ, Chen PS, Chuang SE, Hong CC, Kuo IH, et al. The role of the VEGF-C/VEGFR-3 axis in cancer progression. Br J Cancer 2007;96:541–5.
15. Wang CA, Jedlicka P, Patrick AN, Micalizzi DS, Lemmer KC, Deitsch E, et al. SIX1 induces lymphangiogenesis and metastasis via upregulation of VEGF-C in mouse models of breast cancer. J Clin Invest 2012;122:1895–906.
16. Grau S, Thorsteinsdottir J, von Baumgarten L, Winkler F, Tonn JC, Schichor C. Bevacizumab can induce reactivity to VEGF-C and -D in human brain and tumour derived endothelial cells. J Neurooncol 2011;104:103–12.
17. Li D, Xie K, Ding G, Li J, Chen K, Li H, et al. Tumor resistance to anti-VEGF therapy through up-regulation of VEGF-C expression. Cancer Lett 2014;346:45–52.
18. Levy NS, Chung S, Furneaux H, Levy AP. Hypoxic stabilization of vascular endothelial growth factor mRNA by the RNA-binding protein HuR. J Biol Chem 1998;273:6417–23.
19. Wang J, Guo Y, Chu H, Guan Y, Bi J, Wang B. Multiple functions of the RNA-binding protein HuR in cancer progression, treatment responses and prognosis. Int J Mol Sci 2013;14:10015–41.
20. Brennan SE, Kuwano Y, Alkharouf N, Blackshear PJ, Gorospe M, Wilson GM. The mRNA-destabilizing protein tristetraprolin is suppressed in many cancers, altering tumorigenic phenotypes and patient prognosis. Cancer Res 2009;69:5168–76.
21. Griseri P, Pages G. Regulation of the mRNA half-life in breast cancer. World J Clin Oncol 2014;5:323–34.
22. Essafi-Benkhadir K, Onesto C, Stebe E, Moroni C, Pages G. Tristetraprolin inhibits Ras-dependent tumor vascularization by inducing vascular endothelial growth factor mRNA degradation. Mol Biol Cell 2007;18:4648–58.
23. Grepin R, Ambrosetti D, Marsaud A, Gastaud L, Amiel J, Pedeutour F, et al. The relevance of testing the efficacy of anti-angiogenesis treatments on cells derived from primary tumors: a new method for the personalized treatment of renal cell carcinoma. PLoS ONE 2014;9:e89449.
24. Ebos JM, Mastri M, Lee CR, Tracz A, Hudson JM, Attwood K, et al. Neoadjuvant antiangiogenic therapy reveals contrasts in primary and metastatic tumor efficacy. EMBO Mol Med 2014;6:1561–76.
25. Grepin R, Guyot M, Giuliano S, Boncompagni M, Ambrosetti D, Chamorey E, et al. The CXCL7/CXCR1/2 axis is a key driver in the growth of clear cell renal cell carcinoma. Cancer Res 2014;74:873–83.
26. al-Haj L, Al-Ahmadi W, Al-Saif M, Demirkaya O, Khabar KS. Cloning-free regulated monitoring of reporter and gene expression. BMC Mol Biol 2009;10:20.
27. Gao J, Aksoy BA, Dogrusoz U, Dresdner G, Gross B, Sumer SO, et al. Integrative analysis of complex cancer genomics and clinical profiles using the cBioPortal. Sci Signal 2013;6:pl1.
28. Cerami E, Gao J, Dogrusoz U, Gross BE, Sumer SO, Aksoy BA, et al. The cBio cancer genomics portal: an open platform for exploring multidimensional cancer genomics data. Cancer Discov 2012;2:401–4.
29. Gotink KJ, Broxterman HJ, Honeywell RJ, Dekker H, de Haas RR, Miles KM, et al. Acquired tumor cell resistance to sunitinib causes resistance in a HT-29 human colon cancer xenograft mouse model without affecting sunitinib biodistribution or the tumor microvasculature. Oncoscience 2014;1:844–53.
30. Gotink KJ, Broxterman HJ, Labots M, de Haas RR, Dekker H, Honeywell RJ, et al. Lysosomal sequestration of sunitinib: a novel mechanism of drug resistance. Clin Cancer Res 2011;17:7337–46.
31. Shim M, Song C, Park S, Choi SK, Cho YM, Kim CS, et al. Prognostic significance of platelet-derived growth factor receptor-beta expression in localized clear cell renal cell carcinoma. J Cancer Res Clin Oncol 2015;141:2213–20.
32. Schiefer AI, Mesteri I, Berghoff AS, Haitel A, Schmidinger M, Preusser M, et al. Evaluation of tyrosine kinase receptors in brain metastases of clear cell renal cell carcinoma reveals cMet as a negative prognostic factor. Histopathology 2015;67:799–805.
33. Menke J, Kriegsmann J, Schimanski CC, Schwartz MM, Schwarting A, Kelley VR. Autocrine CSF-1 and CSF-1 receptor coexpression promotes renal cell carcinoma growth. Cancer Res 2012;72:187–200.
34. Giuliano S, Cormerais Y, Dufies M, Grepin R, Colosetti P, Belaid A, et al. Resistance to sunitinib in renal clear cell carcinoma results from sequestration in lysosomes and inhibition of the autophagic flux. Autophagy 2015;11:1891–904.
35. Tiedje C, Ronkina N, Tehrani M, Dhamija S, Laass K, Holtmann H, et al. The p38/MK2-driven exchange between tristetraprolin and HuR regulates AU-rich element-dependent translation. PLoS Genet 2012;8:e1002977.
36. Mahtani KR, Brook M, Dean JL, Sully G, Saklatvala J, Clark AR. Mitogen-activated protein kinase p38 controls the expression and posttranslational modification of tristetraprolin, a regulator of tumor necrosis factor alpha mRNA stability. Mol Cell Biol 2001;21:6461–9.
37. Hitti E, Iakovleva T, Brook M, Deppenmeier S, Gruber AD, Radzioch D, et al. Mitogen-activated protein kinase-activated protein kinase 2 regulates tumor necrosis factor mRNA stability and translation mainly by altering tristetraprolin expression, stability, and binding to adenine/uridine-rich element. Mol Cell Biol 2006;26:2399–407.
38. Griseri P, Bourcier C, Hieblot C, Essafi-Benkhadir K, Chamorey E, Touriol C, et al. A synonymous polymorphism of the Tristetraprolin (TTP) gene, an AU-rich mRNA-binding protein, affects translation efficiency and response to Herceptin treatment in breast cancer patients. Hum Mol Genet 2011;20:4556–68.

39. Sandler H, Stoecklin G. Control of mRNA decay by phosphorylation of tristetraprolin. Biochem Soc Trans 2008;36(Pt 3):491–6.
40. Bex A, Kroon BK, de Bruijn R. Is there a role for neoadjuvant targeted therapy to downsize primary tumors for organ sparing strategies in renal cell carcinoma? Int J Surg Oncol 2012;2012:250479.
41. Sennino B, Ishiguro-Oonuma T, Wei Y, Naylor RM, Williamson CW, Bhagwandin V, et al. Suppression of tumor invasion and metastasis by concurrent inhibition of c-Met and VEGF signaling in pancreatic neuroendocrine tumors. Cancer Discov 2012;2:270–87.
42. Ishikawa Y, Aida S, Tamai S, Akasaka Y, Kiguchi H, Akishima-Fukasawa Y, et al. Significance of lymphatic invasion and proliferation on regional lymph node metastasis in renal cell carcinoma. Am J Clin Pathol 2007; 128:198–207.
43. Sennino B, Ishiguro-Oonuma T, Schriver BJ, Christensen JG, McDonald DM. Inhibition of c-Met reduces lymphatic metastasis in RIP-Tag2 transgenic mice. Cancer Res 2013;73:3692–703.
44. Belum VR, Wu S, Lacouture ME. Risk of hand-foot skin reaction with the novel multikinase inhibitor regorafenib: a meta-analysis. Invest New Drugs 2013;31:1078–86.
45. Enholm B, Paavonen K, Ristimäki A, Kumar V, Gunji Y, Klefstrom J, et al. Comparison of VEGF, VEGF-B, VEGF-C and Ang-1 mRNA regulation by serum, growth factors, oncoproteins and hypoxia. Oncogene 1997;14: 2475–83.
46. Abdelmohsen K, Gorospe M. Posttranscriptional regulation of cancer traits by HuR. Wiley Interdiscip Rev RNA 2010;1:214–29.
47. Govindaraju S, Lee BS. Adaptive and maladaptive expression of the mRNA regulatory protein HuR. World J Biol Chem 2013; 4:111–8.
48. Ronkainen H, Vaarala MH, Hirvikoski P, Ristimaki A. HuR expression is a marker of poor prognosis in renal cell carcinoma. Tumour Biol 2011; 32:481–7.
49. Danilin S, Sourbier C, Thomas L, Lindner V, Rothhut S, Dormoy V, et al. Role of the RNA-binding protein HuR in human renal cell carcinoma. Carcinogenesis 2010;31:1018–26.
50. Cao Y, Hoeppner LH, Bach S, E G, Guo Y, Wang E, et al. Neuropilin-2 promotes extravasation and metastasis by interacting with endothelial alpha5 integrin. Cancer Res 2013;73:4579–90.
51. Caunt M, Mak J, Liang WC, Stawicki S, Pan Q, Tong RK, et al. Blocking neuropilin-2 function inhibits tumor cell metastasis. Cancer Cell 2008; 13:331–42.
52. Cetin B, Gonul II, Buyukberber S, Afsar B, Gumusay O, Algin E, et al. The impact of immunohistochemical staining with ezrin-carbonic anhydrase IX and neuropilin-2 on prognosis in patients with metastatic renal cell cancer receiving tyrosine kinase inhibitors. Tumour Biol 2015;36: 8471–8.
53. Escudier B, Porta C, Bono P, Powles T, Eisen T, Sternberg CN, et al. Randomized, controlled, double-blind, cross-over trial assessing treatment preference for pazopanib versus sunitinib in patients with metastatic renal cell carcinoma: PISCES Study. J Clin Oncol 2014;32: 1412–8.